Original Article

OPEN

Vasoprotective effects of NOX4 are mediated via polymerase and transient receptor potential melastatin 2 cation channels in endothelial cells

Rheure Alves-Lopes[a,e], Silvia Lacchini[c], Karla B. Neves[b,e], Adam Harvey[e], Augusto C. Montezano[d,e], and Rhian M. Touyz[d,e]

Background: NOX4 activation has been implicated to have vasoprotective and blood pressure (BP)-lowering effects. Molecular mechanisms underlying this are unclear, but NOX4-induced regulation of the redox-sensitive Ca^{2+} channel TRPM2 and effects on endothelial nitric oxide synthase (eNOS)-nitric oxide signalling may be important.

Method: Wild-type and LinA3, renin-expressing hypertensive mice, were crossed with NOX4 knockout mice. Vascular function was measured by myography. Generation of superoxide (O_2^-) and hydrogen peroxide (H_2O_2) were assessed by lucigenin and amplex red, respectively, and Ca^{2+} influx by Cal-520 fluorescence in rat aortic endothelial cells (RAEC).

Results: BP was increased in NOX4KO, LinA3 and LinA3/NOX4KO mice. This was associated with endothelial dysfunction and vascular remodelling, with exaggerated effects in NOX4KO groups. The TRPM2 activator, ADPR, improved vascular relaxation in LinA3/NOX4KO mice, an effect recapitulated by H_2O_2. Inhibition of PARP and TRPM2 with olaparib and 2-APB, respectively, recapitulated endothelial dysfunction in NOX4KO. In endothelial cells, Ang II increased H_2O_2 generation and Ca^{2+} influx, effects reduced by TRPM2 siRNA, TRPM2 inhibitors (8-br-cADPR, 2-APB), olaparib and GKT137831 (NOX4 inhibitor). Ang II-induced eNOS activation was blocked by NOX4 and TRPM2 siRNA, GKT137831, PEG-catalase and 8-br-cADPR.

Conclusion: Our findings indicate that NOX4-induced H_2O_2 production activates PARP/TRPM2, Ca^{2+} influx, eNOS activation and nitric oxide release in endothelial cells. NOX4 deficiency impairs Ca^{2+} homeostasis leading to endothelial dysfunction, an effect exacerbated in hypertension. We define a novel pathway linking endothelial NOX4/H_2O_2 to eNOS/nitric oxide through PARP/TRPM2/Ca^{2+}. This vasoprotective pathway is perturbed when NOX4 is downregulated and may have significance in conditions associated with endothelial dysfunction, including hypertension.

Keywords: NOX4, transient receptor potential melastatin-2, polymerase, olaparib, 2-APB, H_2O_2, endothelial dysfunction

Abbreviations: eNOS, endothelial nitric oxide synthase; NADPH, nicotinamide adenine dinucleotide phosphate; RAEC, rat aortic endothelial cells; ROS, reactive oxygen species

INTRODUCTION

In the vasculature, the family of nicotinamide adenine dinucleotide phosphate (NADPH) oxidases (NOX) are important sources of reactive oxygen species (ROS), including superoxide anion (O_2^-) and hydrogen peroxide (H_2O_2) [1]. Initial studies focused on O_2^- generated by NOX1 and NOX2, which, when produced in excess, mediates deleterious effects in the cardiovascular system [2]. Although O_2^- has been shown to induce vasoconstriction, H_2O_2 causes both vasorelaxation and vasoconstriction, depending on the vascular bed and cellular source [3–5]. For example, when produced primarily in vascular smooth muscle cells (VSMCs), H_2O_2 promotes vasoconstriction, whereas endothelial-derived H_2O_2 leads to vasodilation [3–5]. Growing evidence suggests that H_2O_2 may be an endothelium-derived hyperpolarizing factor (EDHF) [6].

In endothelial cells, NOX4 is the most prevalent isoform and, in contrast to other NOX isoforms, which generate superoxide O_2^-, NOX4 produces mainly H_2O_2, which may imply an alternative function for this NOX [7,8]. The protective role of NOX4 in the cardiovascular system has been previously described [9,10]. Compared with wild-type mice, aortas from NOX4-deficient mice exhibit increased

Journal of Hypertension 2023, 41:1389–1400

[a]School of Medicine, Medical Sciences and Nutrition, University of Aberdeen, Aberdeen, [b]Strathclyde Institute of Pharmacy & Biomedical Sciences, University of Strathclyde, Glasgow, UK, [c]Institute of Biomedical Sciences, University of Sao Paulo, Sao Paulo, Brazil, [d]Research Institute of the McGill University Health Centre, McGill University, Montreal, Quebec, Canada and [e]School of Cardiovascular and Metabolic Health, University of Glasgow, Glasgow, UK

Correspondence to Rheure Alves-Lopes, PhD, University of Aberdeen School of Medicine and Dentistry, University of Aberdeen, Polwarth Building, Foresterhill Rd, Aberdeen AB25 2ZD, UK. E-mail: Rheure.Lopes@glasgow.ac.uk

Received 31 August 2022 **Revised** 16 May 2023 **Accepted** 17 May 2023

DOI:10.1097/HJH.0000000000003478

inflammation, vascular remodelling and endothelial dysfunction. This is associated with a reduction in H_2O_2 levels, endothelial nitric oxide synthase (eNOS) expression and nitric oxide production [11]. On the contrary, aorta isolated from transgenic mice with endothelium-targeted NOX4 overexpression, exhibit greater endothelial-dependent vasodilatation and lower blood pressure when compared with wild-type mice. This is associated with increased H_2O_2 production and H_2O_2-induced hyperpolarization. These effects contrast markedly with those reported for other NOXes, which involve superoxide-mediated inactivation of nitric oxide [12]. Thus, endothelial NOX4 might counterregulate the deleterious effects of NOX1 and NOX2 in the vasculature. These effects have been attributed, in part, to the activation of eNOS and nitric oxide production. However, molecular mechanisms linking endothelial NOX4/H_2O_2 to eNOS/NO remain unclear. We propose that the transient receptor potential melastatin 2 (TRPM2) cation channel is important.

TRPM2 is a cation channel permeable to Ca^{2+} and is highly sensitive to changes in intracellular H_2O_2 levels [13–15]. In conditions of oxidative stress, including hypertension, H_2O_2 promotes DNA damage leading to poly (ADP-ribose) polymerase-1 (PARP-1) activation. Upon DNA damage, PARP-1 utilizes NAD^+ as the substrate and catalyzes the addition of mono-ADP-ribose (ADPR) to different acceptor proteins, including TRPM2 [16,17]. H_2O_2 can thus activate TRPM2 either indirectly via ADPR release, which binds to TRPM2 or directly via oxidation of cysteine residues (Cys549) in the channel [18–20]. Once activated, TRPM2 increases Ca^{2+} influx and may regulate eNOS, which is highly regulated by intracellular levels of Ca^{2+} [21]. Therefore, TRPM2 may have a protective effect in endothelial cells via Ca^{2+}-regulated eNOS activation and nitric oxide production. Although TRPM2 channels are present in endothelial cells [22], there is a paucity of information on the functional role of TRPM2 in nitric oxide signalling. As NOX4 is an important source of H_2O_2 in vascular cells, the protective role of this NOX may involve H_2O_2-induced TRPM2 activation, followed by increased Ca^{2+} influx, eNOS activation and nitric oxide release. Here, we tested whether NOX4/H_2O_2 mediates endothelial effects through PARP/TRPM2/Ca^{2+} signalling. Vascular studies were performed in an experimental mouse model of angiotensin II (Ang II)-dependent hypertension and in NOX4 knockout mice and molecular studies were executed in cultured endothelial cells.

MATERIALS AND METHODS

Blood pressure and vascular studies in hypertensive (LinA3) mice crossed with NOX4 knockout mice

Blood pressure measurements and vascular studies were performed in male transgenic mice, which express human renin under the control of the transthyretin promoter (LinA3 mice), their wild-type littermates on a C57BL/6 background, NOX4 knockout mice and LinA3 mice crossed with NOX4 knockout mice (aged 4–5 months). Systemic NOX4-null mice were generated by targeted deletion of the translation initiation site and exons 1 and 2 of the gene. All lines were backcrossed more than 10 generations onto a C57BL/6 background as described previously [23]. Animals were fed *ad libitum*. LinA3 mice develop hypertension throughout their lifespan as we previously described [24]. In Lina3 mice, the human prorenin cDNA is expressed primarily in the liver under the control of a 3-kb region of the transthyretin gene promoter. As a result of genetically clamping renin, activation of the renin-angiotensin-aldosterone system is mildly increased in Lina3 mice, which is associated with a progressive increase in blood pressure [24,25]. Experiments were performed in accordance with the United Kingdom Animals Scientific Procedures Act 1986 and ARRIVE Guidelines and approved by the institutional ethics review committee (70/9021).

SBP was assessed by tail-cuff plethysmography (Visitech Systems model BP-2000-M-6; Apex, North Carolina, USA) as described previously [26]. Mice were trained to the apparatus for 1 week before measurements.

Vascular functional studies were performed in second-order branches (diameter of 150–300 μm) of mesenteric arteries without perivascular fat. Vessels were isolated (2 mm in length) from mice and mounted on a wire myograph as previously described [27] (DMT myograph; ADInstruments Ltd., Oxford, UK). Vessel segments were equilibrated in Krebs Henseleit-modified physiological salt solution (in mmol/l: 120 NaCl, 25 $NaHCO_3$, 4.7 KCl, 1.18 KH_2PO_4, 1.18 $MgSO_4$, 2.5 $CaCl_2$, 0.026 EDTA and 5.5 glucose) at 37°C, continuously bubbled with 95% O_2 and 5% CO_2, pH 7.4. After 30 min of stabilization, the contractile ability of the preparations was assessed by adding KCl (120 mmol/l) to the organ baths. Endothelial integrity was verified by relaxation induced by acetylcholine (10^{-6} mol/l; ACh) in vessels pre-contracted with U46619 (3×10^{-8} mol/l). Preconstriction in response to 3×10^{-8} mmol/l U46619 was not different between the groups. In some experiments, vessels were pretreated for 30 min with TRPM2 inhibitor 2-APB (3×10^{-5} mol/l), PARP inhibitor olaparib (10^{-6} mol/l), TRPM2 activator cADPR (10^{-5} mol/l) and H_2O_2 (10^{-3} mol/l).

Oxidative nucleic acid damage in mouse aorta

Oxidative nucleic acid damage was assessed by 8-OHdG immunofluorescence in the aorta sections. After deparaffinization and hydration, sections were heat treated (1 mmol/l EDTA, pH 8.0) for 15 min in a microwave. Primary 8-hydroxyguanosine antibody incubation (8-OHG, 1:200, Ab10802; Abcam, Cambridge, UK) was performed overnight at 4°C, followed by rinsing in TBS+ 0.05% Tween20, and incubation with secondary antibody (Alexa-fluor-488-conjugated, 1:300, A-11055; Molecular Probes, Eugene, Oregon, USA). Lipofuscin-mediated autofluorescence was removed by using 0.1% Sudan Black B (Sigma, St Louis, Missouri, USA). Slides were mounted using ProLong Gold Anti-fade mounting media containing DAPI (Molecular Probes) for nuclei staining. All sections were analysed in Live Cell Microscope (Zeiss, Cambridge, UK), using fluorescent filters (Alexa-fluor-488 and DAPI), and obtained images for each fluorescent filter. 8-OHG analysis was performed by measuring the intensity of immunofluorescence in Alexa-fluor-488 [CTTF = Integrated Density – (Area of selected tissue X Mean fluorescence of background readings].

Mouse aortic proteoglycan and collagen content

To assess aorta proteoglycan content, the sections were stained with Alcian blue (1% w/v). Total proteoglycan content (%) was measured in the media layer of aorta by bright field analysis using an EVOS XL Microscope (Invitrogen, Thermo Fisher Scientific, Waltham, Massachusetts, USA). All data were quantified by digital image analysis software (ImageJ; NIH, Bethesda, Maryland, USA).

To assess collagen content, aorta sections were stained with picrosirius red (0.1% w/v). Total collagen content (%) was measured in the media layer of the aorta by bright field analysis. To distinguish between mature (red/yellow) and immature (green) collagen fibres, sections were also visualized under polarised light using an Olympus BH-2 microscope (Olympus, Tokyo, Japan). These images were also used to measure the thickness of the aorta wall. Data were quantified by digital image analysis software (ImageJ).

Primary culture rat aortic endothelial cells

Molecular and cellular studies were performed in rat aortic endothelial cells (RAEC) (Sigma R304–05A) and cultured with endothelial cell growth medium (PromoCell – C-22010), supplemented with Endothelial Cell Growth Medium (PromoCell – C-39215) and Penicillin-Streptomycin. Cells were stimulated with Ang II 100 nmol/l to activate vascular signalling pathways. In some experiments, pharmacological inhibitors were added 30 min before Ang II. To inhibit PARP and TRPM2 signalling, we used olaparib (1 μmol/l) and 8-Br-cADPR (1 μmol/l), respectively. NOX4 was inhibited with GKT137831 (10 μmol/l), and to reduce H_2O_2 levels, catalase–polyethylene glycol (1000 units/ml) was used. Some experiments were also performed in the presence of PD 123319, AT_2 receptor antagonist and NOX4 siRNA or TRPM2 siRNA.

Small interfering RNA transfection

RAEC cells were transiently transfected with 50 nmol/l rat TRPM2 Silencer Select Pre-designed siRNA – Ambion (Cat 4390816 – ID s148526) (SF 2B) or with 400 nmol/l rat NOX4 Silencer Select Pre-designed siRNA – Ambion [Cat 4390816 – ID s136995) (SF 2A)]. As a control, it was used Silencer Select Negative Control Ambion (Cat 4390844). Experiments were performed immediately (NOX4) or 2 h (TRPM2) after transfections. Silence efficiency was measured by western blot.

Measurement of cellular reactive oxygen species

NADPH-dependent ROS generation was measured by enhanced lucigenin chemiluminescence, with lucigenin as the electron acceptor and NADPH as the substrate as we previously described [28]. Briefly, RAEC were homogenized in assay buffer (in mmol/l: 50 KH_2PO_4, 1 EGTA and 150 sucrose, pH 7.4). The assay was performed with 100 μl of sample, 1.25 μl of lucigenin (5 μmol/l), 25 μl of NADPH (0.1 mmol/l) and assay buffer to a total volume of 250 μl. Luminescence was measured for 30 cycles of 18 s each by a luminometer (Orion II Microplate Luminometer, Berthold, Germany). Basal readings were obtained before the addition of NADPH to the assay. The reaction was started by the addition of the substrate. Basal and buffer blank values were subtracted from the NADPH-derived luminescence. ROS production was expressed as relative luminescence units (RLU)/μg protein. H_2O_2 was assessed with the Amplex Red assay kit (Molecular Probes, Life Technologies). RAECs were incubated with the reaction mixture according to manufacturer specifications. A microplate reader was used for absorbance at 560 nm. H_2O_2 levels were corrected by the protein concentration of each sample.

Measurement of intracellular Ca^{2+} transients

Intracellular free Ca^{2+} levels were measured in RAEC using the fluorescent Ca^{2+} indicator, Cal-520 acetoxymethyl ester (Cal-520/AM; Abcam; 10 μmol/l). Fluorescence measurements were performed using an inverted epifluorescence microscope (Axio Observer Z1 Live-Cell imaging system; Zeiss) with excitatory wavelengths of 490 and emission of 535. Images were acquired and analysed using Zen Blue Program (Zeiss). Cells were grown in six-well plates and following the removal of culture media were incubated with 10 μmol/l of Cal-520 AM in 0.5% FBS at 37°C for 75 min followed by 30 min at room temperature. Following incubation, the dye solution was replaced with HEPES physiological saline solution containing the following components (in mmol/l): NaCl 130, KCl 5, CaCl 1, MgCl 1, HEPES 20 and D-glucose 10, pH 7.4) for 30 min before imaging. Fluorescence intensity as a measure of $[Ca^{2+}]i$, was monitored for 30 s in basal condition and 2.5 min under Ang II 10^{-7} mol/l stimulation.

Immunoblotting

Total protein was extracted from RAEC, which were lysed in 50 mmol/l Tris-HCl (pH 7.4) lysis buffer containing 1% Nonited P-40, 0.5% sodium deoxycholate, 150 mmol/l NaCl, 1 mmol/l EDTA, 0.1% SDS, 2 mmol/l sodium orthovanadate (Na_3VO_4), 1 mmol/l phenylmethylsulfonyl fluoride (PMSF), 1 μg/ml pepstatin A, 1 μg/ml leupeptin and 1 μg/ml aprotinin. Total protein extract was sonicated and cleared by centrifugation at 10 000 rpm for 10 min and pellet containing mostly debris and non lysed cells, was discarded. Protein concentrations were determined using the DC protein assay kit (Bio-Rad Laboratories, Hercules, California, USA). Proteins from homogenates (30 μg) were separated by electrophoresis on a polyacrylamide gel and transferred onto a nitrocellulose membrane. Nonspecific binding sites were blocked with 3% bovine serum albumin in Tris-buffered saline solution with 0.1% Tween for 1 h at room temperature. Membranes were then incubated with specific antibodies overnight at 4°C. Antibodies used were Anti-NOX 4 (abcam - ab133303 – 1:1000), Anti-TRPM2 (Abcam – ab96785 – 1:10000), Phospho-eNOS (Ser1177) (cell Signaling - 9571l – 1:1000) and loading control GAPDH (Abcam - ab8245 – 1:5000). After incubation (1 h) with secondary fluorescence-coupled antibodies (Licor), signals were visualized by an infrared laser scanner (Odyssey Clx, LICOR). Protein expression levels were normalized to loading controls and expressed as a percentage (%) of the control.

PARP activity

PARP activity was assessed based on the detection of biotinylated poly (ADP-ribose) deposited by PARP-1 onto immobilized histones (Trevigen 4677-096-K). About

40–60 μg of protein from cell lysates were loaded into a 96-well plate coated with histones and biotinylated polyADPribose, allowed to incubate for 1 h, treated with strep-HRP and read at 450 nm in a spectrophotometer.

Nitric oxide production

Production of nitric oxide was determined using the nitric oxide fluorescent probe diacetate 4-amino-5-methylamino-2',7'-difluorofluorescein diacetate (DAF-FM; Life Technologies, Molecular Probes, Paisley, UK). RAEC were loaded with DAF-FM diacetate (final concentration 5 μmol/l, 30 min) in serum-free media, kept in the dark and maintained at 37°C, as we previously described [29]. Briefly, cells were washed to remove the exceeding probe. The medium was replaced and incubated for an additional 10 min to allow complete de-esterification of the intracellular diacetates. Nitric oxide levels were assessed in the presence and absence of GKT 137831 (10^{-5} mol/l) and 8-Br-cADPR (10^{-6} mol/l). Cells were washed with phosphate-buffered saline (PBS) and harvested with mild trypsinization at 0.025%. Trypsin was inactivated with soybean trypsin inhibitor (0.025%) in PBS (1:1). After washing, the pellet was transferred to a black 96 well microplate (BD Falcon, Loughborough, UK). The DAF-FM fluorescence was assessed with a spectrofluorometer at excitation/emission wavelengths of 495/515 nm. Fluorescence intensity was normalized to the protein concentration and expressed as fluorescence emission/μg of protein.

Statistical analysis

For vascular functional studies, concentration-response curves were generated, and the maximal effect (E_{max}) was calculated using nonlinear regression analysis. pD_2 (defined as the negative logarithm of the EC_{50} values) and E_{max} were compared by Student's *t*-test or two-way analysis of variance (ANOVA) with Bonferroni post-test, as appropriate. For the other experiments, statistical comparisons between groups were performed using a two-tailed Student's *t*-test and or one-way ANOVA. Bonferroni or Dunnett post-test were used as appropriate. A P value less than 0.05 was considered statistically significant. Data analysis was conducted using GraphPad Prism 8.0 (GraphPad Software Inc., San Diego, California, USA). Data are expressed as mean ± SEM.

RESULTS

Increased blood pressure and vascular dysfunction in mice deficient in NOX4

Blood pressure was significantly increased in LinA3 mice, NOX4KO mice and LinA3/NOX4KO mice versus controls ($P < 0.05$) (Fig. 1a). Aorta from LinA3/NOX4KO mice exhibited increased thickness with associated increase in collagen and proteoglycan content versus wild-type (Figure 1b–d). This was also associated with increased oxidative DNA damage, as assessed by 8-OHdG, a biomarker for the measurement of ROS-induced DNA damage [30] (Supplementary Figure 2; http://links.lww.com/HJH/C206).

Mesenteric arteries isolated from hypertensive LinA3 mice exhibit reduced endothelial function (Fig. 2a), an effect exacerbated in the absence of NOX4 (Fig. 2b). To explore the potential role of TRPM2, H_2O_2 and PARP-1 in endothelial dysfunction, vessels were pre-treated with modulators of TRPM2 (cADPR, TRPM2 activator; 2-APB, TRPM2 inhibitor), PARP-1 (olaparib, PARP inhibitor) and H_2O_2. As shown in Fig. 2c, cADPR ameliorated endothelial dysfunction observed in LinA3/NOX4KO mice. These effects were recapitulated in vessels exposed to H_2O_2 (Fig. 2d). Olaparib induced a slight but significant impairment in endothelial function in LinA3 vessels (Fig. 2e), while 2-APB worsened endothelium-dependent vasorelaxation in wild-type and LinA3 mice (Fig. 2f).

Ang II-induced reactive oxygen species generation and PARP activation in endothelial cells are NOX4-dependent

To explore in greater detail putative molecular mechanisms and NOX4-dependent processes observed in intact vessels, we measured NOX-induced ROS production by assessing NADPH-dependent O_2^- generation and H_2O_2 levels via lucigenin chemiluminescence and amplex red assay respectively. As demonstrated in Fig. 3a and b, stimulation with Ang II for 5 min induced ROS generation in RAEC. To assess the role of NOX4, experiments were performed in the presence of NOX4 siRNA (Fig. 3g). Figure 3c and d show that Ang II-induced ROS generation in RAEC is reduced in the absence of NOX4. ROS generation and H_2O_2 production induced by Ang II were reversed in the presence of the AT_2 receptor antagonist PD 123 319 and NOX4 inhibitor GKT 137831 (Fig. 3e and f).

In conditions of oxidative stress, H_2O_2 can cause DNA damage, leading to PARP activation. To assess this in RAEC, cells were stimulated with Ang II and PARP activity was measured. As observed in Fig. 4a, Ang II significantly increased PARP activation. This was abolished when cells were pre-treated with GKT137831, and PEG-Catalase, which dismutates H_2O_2. Activation of PARP induced by Ang II was blunted by NOX4 siRNA (Fig. 4b).

Ca^{2+} influx in rat aortic endothelial cells induced by Ang-II is dependent on NOX4, PARP and TRPM2 signalling

To assess whether NOX4/PARP/TRPM2 signalling plays a role in Ang II-induced Ca^{2+} influx in RAEC, cells were pretreated with GKT137831, PEG-catalase (reduces H_2O_2 levels), 8-Br-cADPR and 2-APB (TRPM2 inhibitors) and Olaparib (PARP inhibitor). Enhanced Ang-II induced Ca^{2+} influx in RAEC was reduced in the presence of NOX4/PARP/TRPM2 inhibitors (Fig. 5a–c). Corroborating the pharmacological data, NOX4siRNA and TRPM2 siRNA also reduced Ang II-induced Ca^{2+} influx in RAEC (Fig. 5d–f). Non-targeting siRNA had no impact on Ang II-induced Ca^{2+} influx in RAECs (Supplementary Figure 1; http://links.lww.com/HJH/C206).

NOX4 and redox-sensitive TRPM2 channels are involved in Ang-II induced endothelial nitric oxide synthase activation

Phosphorylation of eNOS is regulated by Ca^{2+} and it is an important step involved in vascular relaxation [31]. Considering the involvement of NOX4/TRPM2 signalling in enhanced Ca^{2+} influx in RAEC, we next evaluated whether eNOS phosphorylation in cells stimulated with Ang II

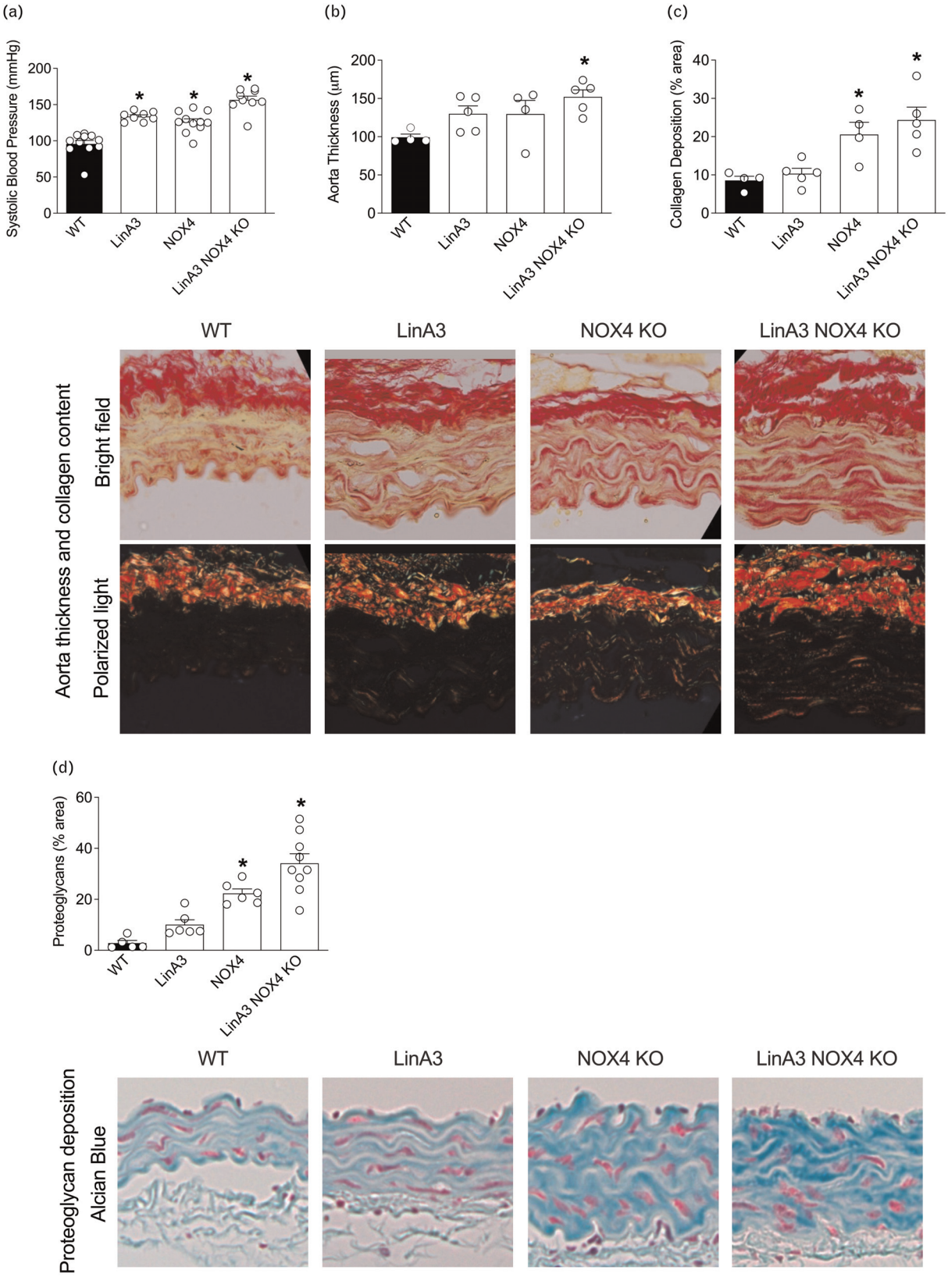

FIGURE 1 SBP was assessed by tail-cuff plethysmography (a). For collagen deposition, aortas were isolated from control, LinA3, NOX4KO and LinA3/NOX4 KO mice. Bar graphs represent aorta thickness (b) and collagen content (c). To distinguish between mature (red/yellow) and immature (green) collagen fibres, sections were also visualized under polarized light using. These images were also used to measure the thickness of the aorta wall. Aortas were isolated from control, LinA3, NOX4KO and LinA3/NOX4 KO mice. Proteoglycan content in aorta was assessed by Alcian blue staining (1% w/v) (d). Data are mean ± SEM ($n = 4–11$). $P < 0.05$. [a] versus WT.

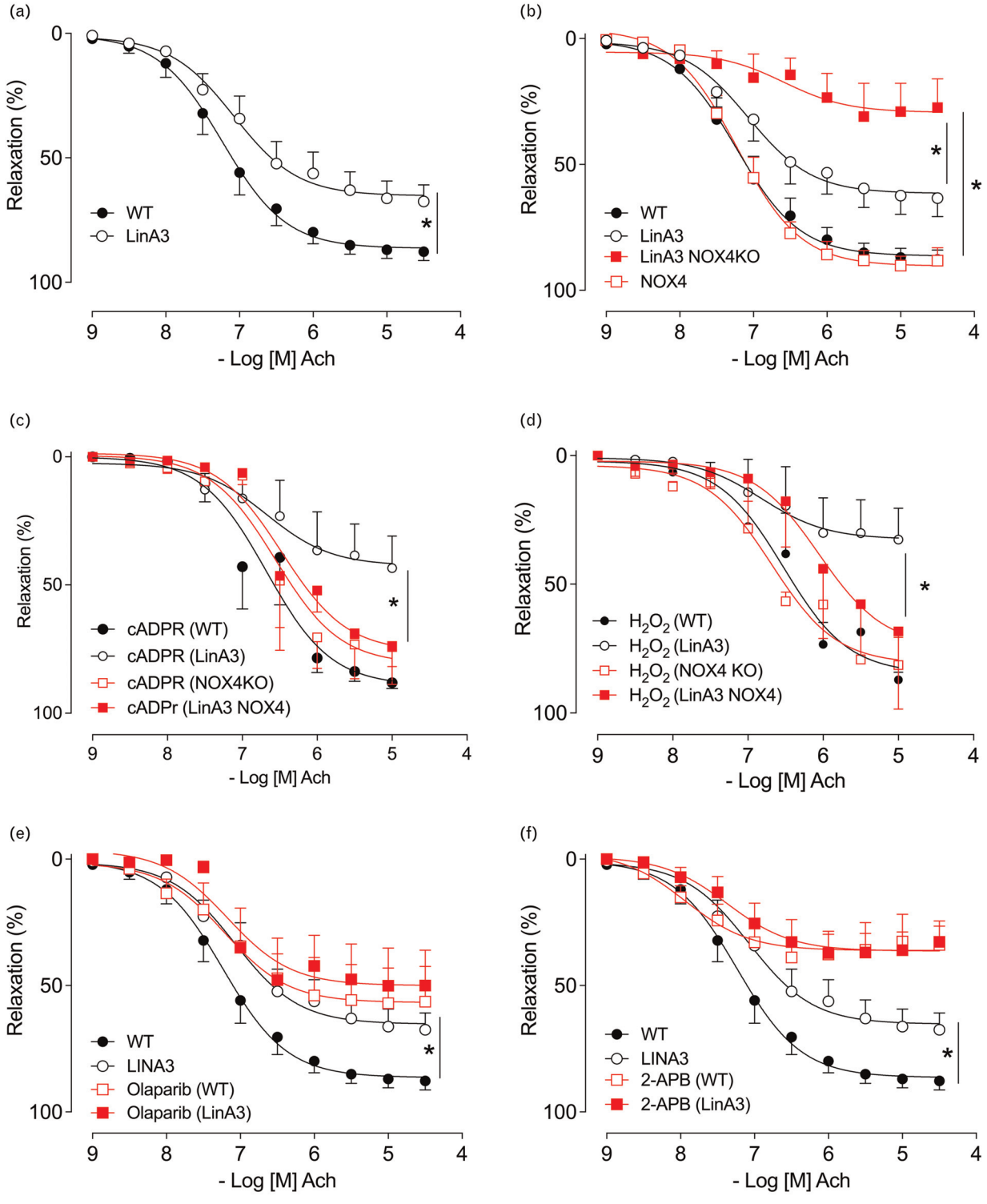

FIGURE 2 Concentration-response curves to ACh were performed in mesenteric arteries isolated from wild-type (WT), LinA3, WT/NOX4 knockout (KO) mice and LinA3/NOX4 KO mice and mounted on wire myograph in the presence and absence of TRPM2 activator cADPR (10^{-5} mol/l) H_2O_2 (10^{-3} mol/l), olaparib (10^{-6} mol/l) and 2-APB (3×10^{-5} mol/l). When used, drugs were preincubated 30 min before the concentration-response curves. Vessels were pre-contracted with U46619 (3×10^{-8} mol/l) and cumulative concentration-response curves to ACh (relaxation) were performed. Curves are represented in nonlinear regression ± SEM ($n = 6$-8). *$P < 0.05$ versus WT.

involves NOX4 and TRPM2 (Fig. 6a–e). Ang II induced a significant increase in eNOS phosphorylation, with maximal responses at 5 min (Fig. 6a). Pretreatment of cells with NOX4 (GKT137831) and TRPM2 (8-Br-cADPR) inhibitors attenuated Ang II-stimulated phosphorylation of eNOS (Fig. 6b) and nitric oxide release (Fig. 6e) in RAEC. This was recapitulated when NOX4 and TRPM2 were down-regulated with siRNA (Fig. 6c and d).

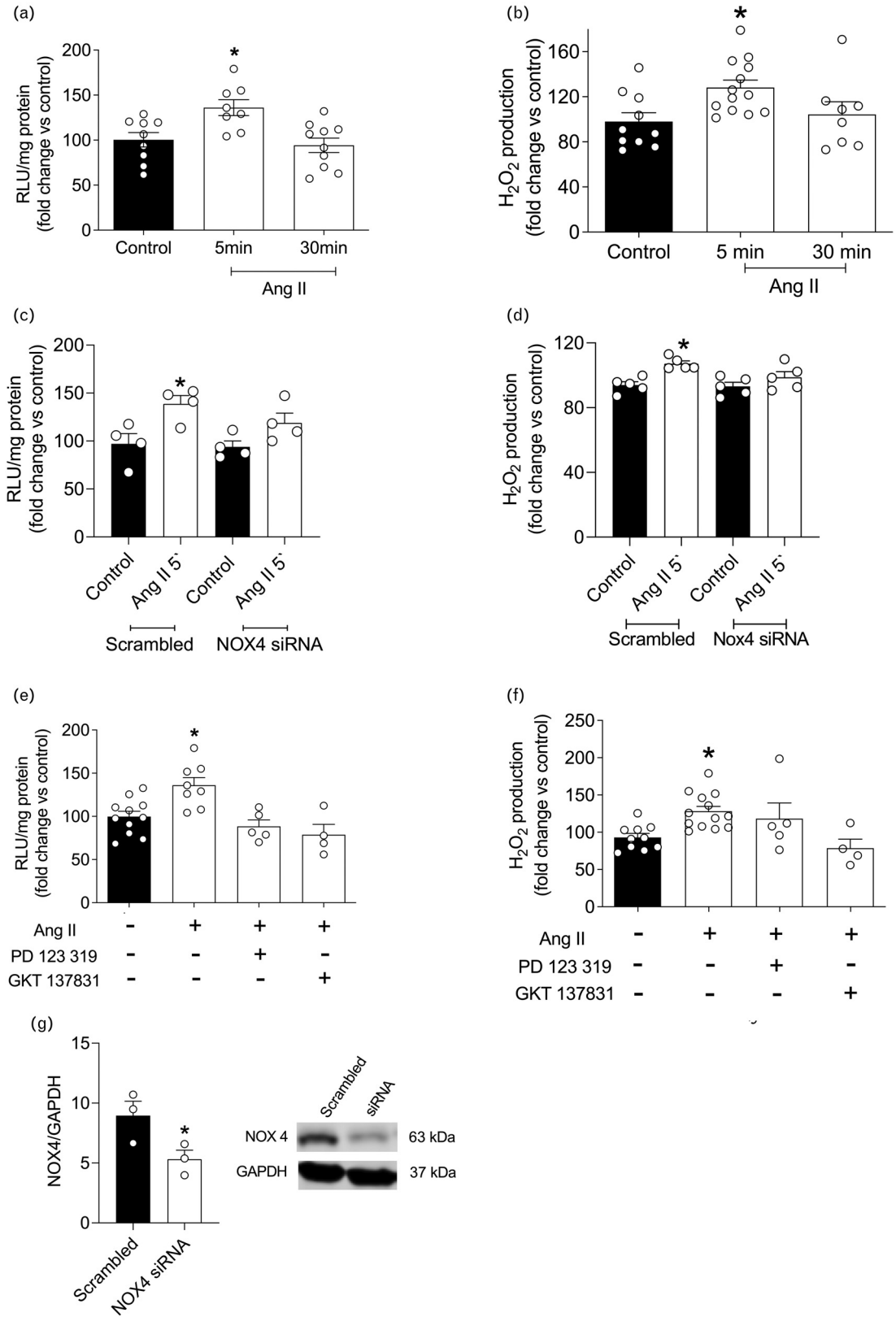

FIGURE 3 ROS generation was measured in rat aortic endothelial cells (RAEC) stimulated with Ang II (10^{-7} mol/l) by lucigenin (a, c, e), and H_2O_2 (b, d, f) generation via Amplex Red assay. When used, AT_2 receptor antagonist (PD 123319 – 10^{-6} mol/l) and NOX1/NOX4 inhibitor (GKT 137831 - 10^{-5} mol/l) were added 30 min prior experiment. RAEC cells were transiently transfected for 6 h with 400 nmol/l rat NOX4 Silencer Select Pre-designed siRNA. As a control, Silencer Select Negative Control Ambion was used. Experiments were performed immediately after transfections (g). As a control, Silencer Select Negative Control Ambion was used. Experiments were performed immediately after transfections. Bars represent the mean ± SEM ($n = 4–11$). $^*P < 0.05$ versus Control.

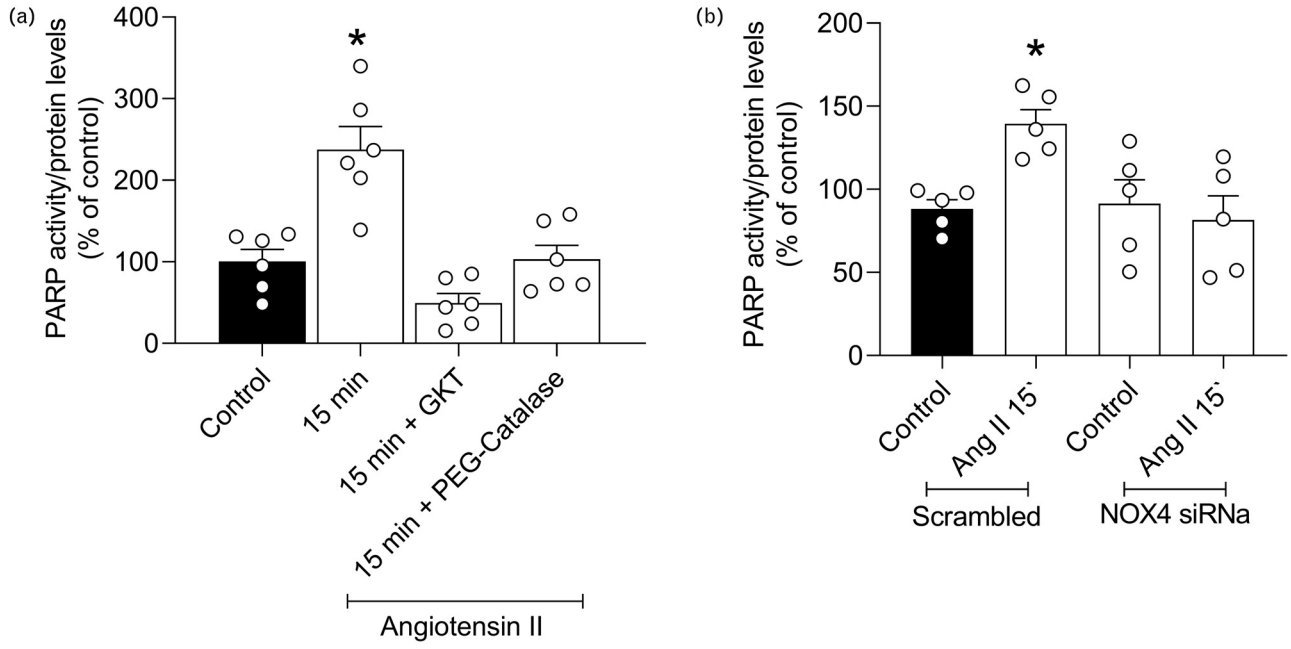

FIGURE 4 PARP activity was assessed based on the incorporation of biotinylated ADP-ribose to histone proteins in RAEC in basal conditions or stimulated with Ang II (15 min) in the presence or absence of GKT 137831 (10^{-5} mol/l), PEG-Catalase (1000 units/ml) (a) and NOX4 siRNA (b). Cells were pre-treated with GKT 137831 or PEG-Catalase for 30 min or transfected with NOX4 siRNA for 6 h, and experiments were performed right after pre-treatment/transfection. Bars represent the mean ± SEM ($n = 5–6$). $^*P < 0.05$. versus Control.

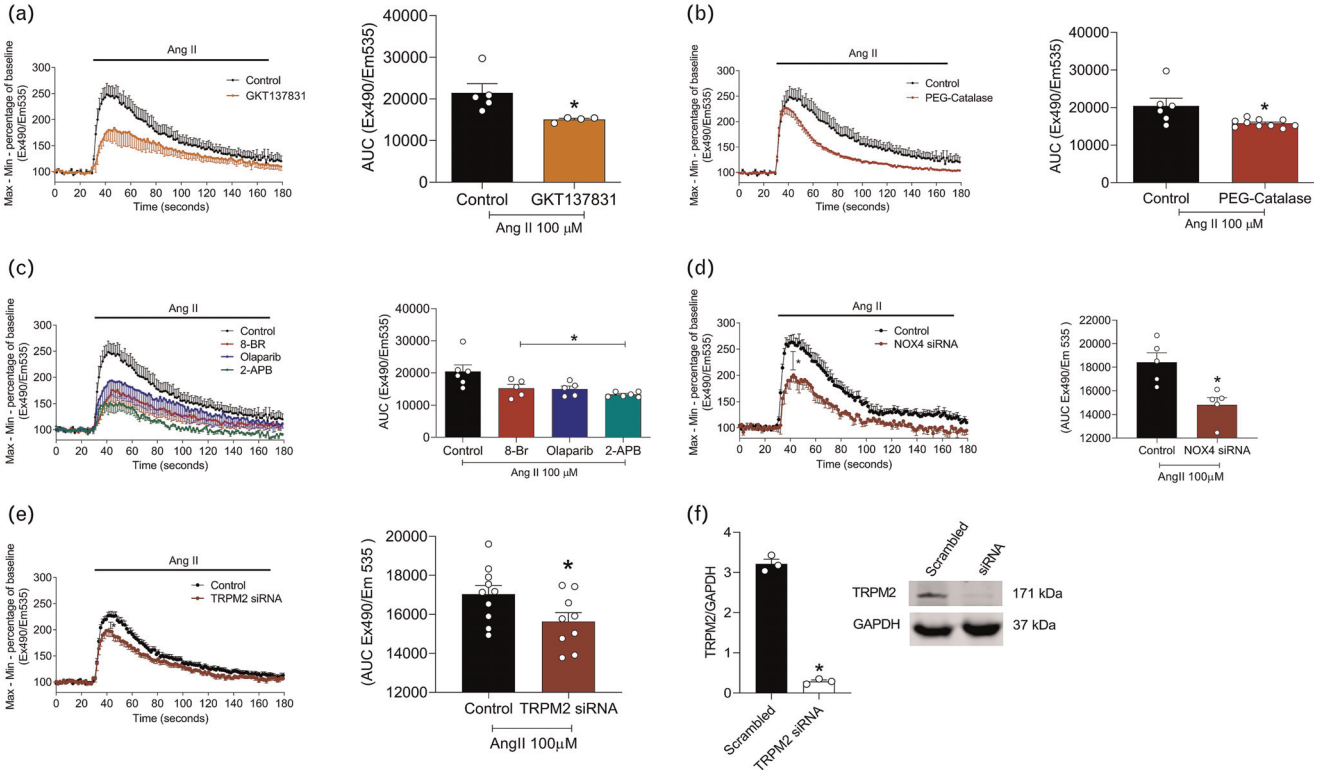

FIGURE 5 Ca^{2+} influx (Cal-520 AM) was measured in RAEC. The influx of Ca^{2+} was assessed by measuring $[Ca^{2+}]_i$ in the absence (30 s) and presence of Ang II 10^{-7} mol/l (2.5 min). Bar graphs are presented as the area under the curve (AUC). Cells were pre-treated with GKT 137831 (10^{-5} mol/l) (a), PEG-Catalase (1000 units/ml) (b), 8-Br-cADPR (10^{-6} mol/l), Olaparib (10^{-6} mol/l), 2-APB (3×10^{-5} mol/l) (c). Ca^{2+} influx was also assessed in presence of NOX4 (400 nmol/l) and TRPM2 siRNA (50 nmol/l) (e, f). RAEC cells were transiently transfected for 6 h with 50 nmol/l rat TRPM2 Silencer Select Pre-designed siRNA or with 400 nmol/l rat NOX4 Silencer Select Pre-designed siRNA. As a control, Silencer Select Negative Control Ambion was used. Experiments were performed immediately (NOX4) or 2 h (TRPM2) after transfections. Bars represent the area under the curve ± SEM ($n = 4–6$). $^*P < 0.05$ versus Control.

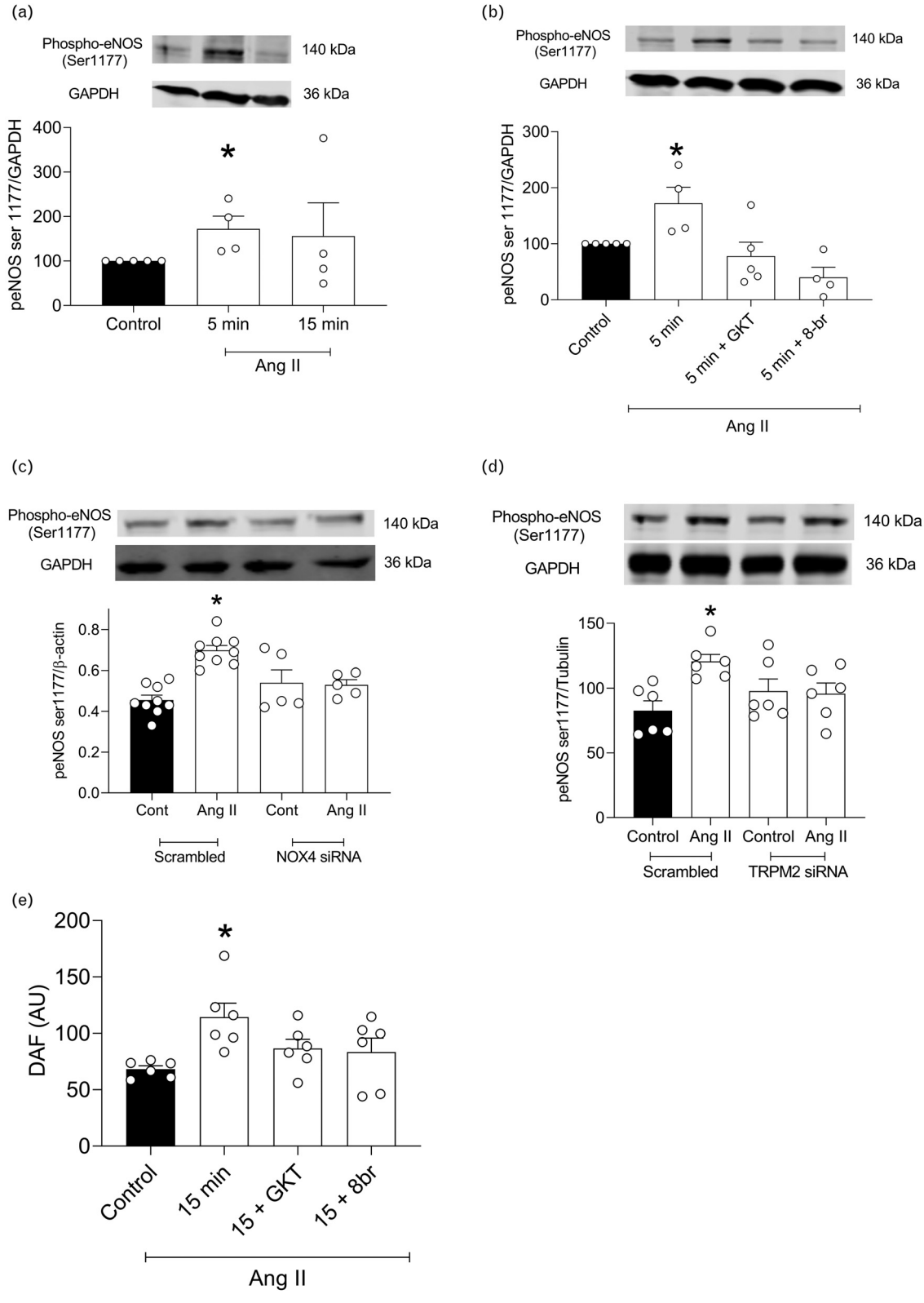

FIGURE 6 Phosphorylation of eNOS (a–d) (Ser1177) was assessed by western blot in RAEC and normalized by GAPDH expression, and nitric oxide detection by DAF-FM Diacetate (4-Amino-5-Methylamino-2′,7′-Difluorofluorescein Diacetate) fluorescence. Experiments were done in the presence and absence of GKT 137831 (10^{-5} mol/l), 8-Br-cADPR (10^{-6} mol/l), NOX4 (400 nmol/l) and TRPM2 siRNA (50 nmol/l). Cells were pre-treated with inhibitors for 30 min or transiently transfected for 6 h with 50 nmol/l rat TRPM2 Silencer Select Pre-designed siRNA or with 400 nmol/l rat NOX4 Silencer Select Pre-designed siRNA. As a control, Silencer Select Negative Control Ambion was used. Experiments were performed immediately (NOX4) or 2 h (TRPM2) after transfections. Bars represent the mean ± SEM ($n = 4–9$). $*P < 0.05$ versus Control.

DISCUSSION

Major findings from the present study demonstrate that NOX4 deficiency is associated with hypertension and potentiation of endothelial dysfunction and vascular remodelling in a mouse model of hypertension. To unravel molecular mechanisms underlying these phenomena, studies were performed in cultured endothelial cells, where Ang II, via AT2R, induced generation of H_2O_2 and activation of TRPM2, with consequent increase in Ca^{2+} influx, activation of eNOS and release of nitric oxide, which causes vascular relaxation. Our findings identify a novel pathway involving NOX4/H_2O_2-modulation of redox-sensitive TRPM2 channels in endothelial cells, which influences cellular Ca^{2+} homeostasis, important in the regulation of nitric oxide production, endothelial function and blood pressure control.

NOX4 is the major NOX isoform expressed in endothelial cells [32,33], and in contrast to other NOXs, which generate O_2^-, NOX4 activation leads to production of H_2O_2 [34]. Transgenic overexpression of NOX4 in the vascular endothelium of mice enhances endothelial-dependent relaxation, followed by a reduction in blood pressure, with no effects on endothelial-independent relaxation or vascular contractility, suggesting that NOX4 protective effects are unique to endothelial cells [12]. Improvement of relaxation in transgenic NOX4 mice is abolished in the presence of catalase, which scavenges H_2O_2, indicating that enhanced vasodilatation induced by overexpression of NOX4 is dependent on H_2O_2 generation [12]. Our findings further support this, as blood pressure in NOX4 knockout mice was elevated to similar levels to that in LinA3 mice, a model of Ang II-dependent hypertension. Moreover, we clearly demonstrate that the pressor effect of NOX4/H_2O_2 deficiency is linked to endothelial dysfunction, oxidative DNA damage and ECM remodelling. Together, these findings suggest that NOX4/H_2O_2 has blood pressure depressor and vasoprotective effects.

Ang II increased endothelial cell H_2O_2 generation through AT_2R, as effects were attenuated in cells pre-exposed to the AT2R antagonist PD123319. Agonist-stimulated H_2O_2 production was also reduced in endothelial cells in which NOX4 activity was inhibited pharmacologically and by siRNA downregulation. These findings corroborate previous publications indicating that NOX4 generates primarily H_2O_2 [34–36]. Several articles have reported NOX4/H_2O_2 functional effects in endothelial cells. NOX4 overexpression potentiates endothelial proliferation, increases tube formation, cell migration and eNOS expression, effects reversed by antioxidant agents [37,38]. In the presence of nitric oxide, NOX4 overexpression does not lead to injurious peroxynitrite ($ONOO^-$) formation [7,39]. Mechanisms by which NOX4 induction of H_2O_2 production modulate endothelial function are elusive, but may be associated with the PARP-regulated Ca^{2+}-permeable channel TRPM2, as we demonstrate here. We showed that in Ang II stimulated endothelial cells, PARP is activated in a NOX4/H_2O_2-dependent manner. Supporting our paradigm, others have suggested a role for PARP activation in endothelial cells. This was shown in endothelial cells exposed to hypoxia wherein redox-regulated Ca^{2+} influx and ERK1/2 activation were reduced by PARP inhibition [40]. Together, these findings suggest that PARP is downstream of NOX/ROS formation and a prerequisite for redox-regulated Ca^{2+} homeostasis.

In TRPM2-overexpressing cells, PARP inhibitors prevent ROS-induced Ca^{2+} influx [41], a paradigm that we further explored in endothelial cells. To inhibit TRPM2 and NOX4 signalling, we used several pharmacological agents that modulate TRPM2, PARP and NOX: 2-APB is a TRPM2 channel blocker, olaparib is a PARP inhibitor, 8-Br-cADPR is a cyclic ADP-ribose inhibitor and GKT137831 inhibits NOX/ NOX4. Although these agents may have some non-specificity, we further verified TRPM2 and NOX4 using siRNA. We observed that Ca^{2+} transients induced by Ang II in RAEC is an event dependent on NOX4, H_2O_2, PARP and TRPM2 Ca^{2+} channel. These data suggest that oxidative stress via PARP activation may lead to Ca^{2+} influx via TRPM2.

As eNOS activation is regulated by Ca^{2+} levels, we next sought to determine whether the final downstream target of this cascade is activation of eNOS, resulting in the production of nitric oxide, a potent vasodilator [42]. We observed that Ang II induces eNOS activation in endothelial cells followed by an increase in nitric oxide release, an effect dependent on NOX4 and TRPM2. Our data identify eNOS as a downstream component of NOX4/TRPM2 signalling. As eNOS and its production of bioactive nitric oxide contribute to vasodilation [42], mice lacking NOX4 exhibit significant impairment in TRPM2 signalling with a consequent reduction in Ca^{2+} influx followed by endothelial dysfunction. Our findings suggest that activation of the NOX4/H_2O_2/PARP/TRPM2 pathway regulates nitric oxide dependent relaxation, promoting cardiovascular protective effects [11,43]. Similar results have been observed in porcine aortic endothelial cells, wherein H_2O_2 regulates eNOS Ser-1177 phosphorylation [44].

The functional significance of these molecular systems was demonstrated in the studies on intact arteries isolated from wild-type, NOX4 knockout mice, LinA3/NOX4 knockout mice and LinA3 mice, which recapitulate human hypertension [45]. Endothelial-dependent relaxation was reduced in LinA3 hypertensive mice, similar to what has been previously described in models of Ang II induced hypertension [46–48]. Impairment in endothelial-dependent relaxation was potentiated in the absence of NOX4 (LinA3NOX4 mice) but attenuated when LinA3/NOX4 knockout vessels were treated with activators of TRPM2 and H_2O_2. On the contrary, pharmacological inhibition of PARP and TRPM2 recapitulated vascular dysfunction that was observed in the absence of NOX4. Together our in-vitro and ex-vivo studies highlight an important role for NOX4/H_2O_2 regulation of PARP-TRPM2 modulation of Ca^{2+} that contributes to eNOS activation and nitric oxide release in endothelial cells.

In addition to endothelial cells, TRPM2 has been studied in VSMCs [15]. Previous findings suggest that in hypertension, oxidative stress promotes activation of TRPM2 in VSMCs leading to perturbed Ca^{2+} handling and increased vascular contractility [15]. Although TRPM2 may have a hypercontractile effect in VSMCs, we demonstrate here that, in endothelial cells, TRPM2 activation via regulation

of Ca^{2+} homeostasis, leads to eNOS-induced nitric oxide release and vascular relaxation. Together, these data suggest diverse functional and cellular effects of TRPM2. The distinct effects of TRPM2 may be associated with different signalling pathways regulated by Ca^{2+}. For example, in VSMCs, Ca^{2+}-mediated activation of myosin light chain leads to vasoconstriction, whereas Ca^{2+}-mediated activation of eNOS in endothelial cells causes vasorelaxation [21,49]. In-vivo studies, wherein hypertensive animals are treated with TRPM2 inhibitors, will better elucidate the role of this channel in pathophysiological conditions.

In conclusion, we define a novel molecular pathway in endothelial cells, wherein NOX4-induced H_2O_2 production activates PARP/TRPM2 signalling with associated increase in Ca^{2+} influx, eNOS activation and nitric oxide release (Supplementary Figure 3; http://links.lww.com/HJH/C206). The absence of NOX4 impairs Ca^{2+} homeostasis leading to endothelial dysfunction, an effect exacerbated in a pathological condition such as hypertension. Taking into consideration the cardiovascular deleterious effects induced by other isoforms of the NOX family, our data suggest that future potential therapeutic strategies to modulate ROS production in cardiovascular diseases need to target individual NOX isoforms, preferably in a cell-specific manner, rather than global inhibition of NOXs.

ACKNOWLEDGMENTS

The authors thank Wendy Beattie for help with the mouse colonies and blood pressure measurement; Laura Haddow and John McAbeny for technical support in the myography facility; and the BHF Myography & Imaging Core Facility.

This study was supported by grants from the British Heart Foundation (BHF) (RE/13/5/30177; 18/6/34217; CH/12/29762) and Tenovus Scotland (316121-01). A.C.M. was supported through a Walton Foundation fellowship, University of Glasgow. R.M.T. is supported by grants from the Leducq Foundation, Dr Phil Gold Chair, McGill University and the European Commission.

Conflict of interest

None.

REFERENCES

1. Panday A, Sahoo MK, Osorio D, Batra S. NADPH oxidases: an overview from structure to innate immunity-associated pathologies. *Cell Mol Immunol* 2015; 12:5–23.
2. Cave AC, Brewer AC, Narayanapanicker A, Ray R, Grieve DJ, Walker S, *et al*. NADPH oxidases in cardiovascular health and disease. *Antioxid Redox Signal* 2006; 8:691–728.
3. Byon CH, Heath JM, Chen Y. Redox signaling in cardiovascular pathophysiology: a focus on hydrogen peroxide and vascular smooth muscle cells. *Redox Biol* 2016; 9:244–253.
4. Feelisch M, Akaike T, Griffiths K, Ida T, Prysyazhna O, Goodwin JJ, *et al*. Long-lasting blood pressure lowering effects of nitrite are NO-independent and mediated by hydrogen peroxide, persulfides, and oxidation of protein kinase G1alpha redox signalling. *Cardiovasc Res* 2020; 116:51–62.
5. Lucchesi PA, Belmadani S, Matrougui K. Hydrogen peroxide acts as both vasodilator and vasoconstrictor in the control of perfused mouse mesenteric resistance arteries. *J Hypertens* 2005; 23:571–579.
6. Matoba T, Shimokawa H, Nakashima M, Hirakawa Y, Mukai Y, Hirano K, *et al*. Hydrogen peroxide is an endothelium-derived hyperpolarizing factor in mice. *J Clin Invest* 2000; 106:1521–1530.
7. Takac I, Schroder K, Zhang L, Lardy B, Anilkumar N, Lambeth JD, *et al*. The E-loop is involved in hydrogen peroxide formation by the NADPH oxidase Nox4. *J Biol Chem* 2011; 286:13304–13313.
8. Langbein H, Shahid A, Hofmann A, Mittag J, Bornstein SR, Morawietz H, *et al*. NADPH oxidase 4 mediates the protective effects of physical activity against obesity-induced vascular dysfunction. *Cardiovasc Res* 2020; 116:1767–1778.
9. Schurmann C, Rezende F, Kruse C, Yasar Y, Lowe O, Fork C, *et al*. The NADPH oxidase Nox4 has anti-atherosclerotic functions. *Eur Heart J* 2015; 36:3447–3456.
10. Langbein H, Brunssen C, Hofmann A, Cimalla P, Brux M, Bornstein SR, *et al*. NADPH oxidase 4 protects against development of endothelial dysfunction and atherosclerosis in LDL receptor deficient mice. *Eur Heart J* 2016; 37:1753–1761.
11. Schroder K, Zhang M, Benkhoff S, Mieth A, Pliquett R, Kosowski J, *et al*. Nox4 is a protective reactive oxygen species generating vascular NADPH oxidase. *Circ Res* 2012; 110:1217–1225.
12. Ray R, Murdoch CE, Wang M, Santos CX, Zhang M, Alom-Ruiz S, *et al*. Endothelial Nox4 NADPH oxidase enhances vasodilatation and reduces blood pressure in vivo. *Arterioscler Thromb Vasc Biol* 2011; 31:1368–1376.
13. Uemura T, Kudoh J, Noda S, Kanba S, Shimizu N. Characterization of human and mouse TRPM2 genes: identification of a novel N-terminal truncated protein specifically expressed in human striatum. *Biochem Biophys Res Commun* 2005; 328:1232–1243.
14. Owsianik G, Talavera K, Voets T, Nilius B. Permeation and selectivity of TRP channels. *Annu Rev Physiol* 2006; 68:685–717.
15. Alves-Lopes R, Neves KB, Anagnostopoulou A, Rios FJ, Lacchini S, Montezano AC, *et al*. Crosstalk between vascular redox and calcium signaling in hypertension involves TRPM2 (transient receptor potential melastatin 2) cation channel. *Hypertension* 2020; 75:139–149.
16. Sousa FG, Matuo R, Soares DG, Escargueil AE, Henriques JA, Larsen AK, *et al*. PARPs and the DNA damage response. *Carcinogenesis* 2012; 33:1433–1440.
17. Wei H, Yu X. Functions of PARylation in DNA damage repair pathways. *Genomics Proteomics Bioinformatics* 2016; 14:131–139.
18. Ru X, Yao X. TRPM2: a multifunctional ion channel for oxidative stress sensing. *Sheng Li Xue Bao* 2014; 66:7–15.
19. Wang G, Cao L, Liu X, Sieracki NA, Di A, Wen X, *et al*. Oxidant sensing by TRPM2 inhibits neutrophil migration and mitigates inflammation. *Dev Cell* 2016; 38:453–462.
20. Keckeis S, Wernecke L, Salchow DJ, Reichhart N, Strauss O. Activation of a Ca(2+)-dependent cation conductance with properties of TRPM2 by reactive oxygen species in lens epithelial cells. *Exp Eye Res* 2017; 161:61–70.
21. Lin S, Fagan KA, Li KX, Shaul PW, Cooper DM, Rodman DM. Sustained endothelial nitric-oxide synthase activation requires capacitative Ca2+ entry. *J Biol Chem* 2000; 275:17979–17985.
22. Hecquet CM, Ahmmed GU, Vogel SM, Malik AB. Role of TRPM2 channel in mediating H2O2-induced Ca2+ entry and endothelial hyperpermeability. *Circ Res* 2008; 102:347–355.
23. Zhang M, Brewer AC, Schroder K, Santos CX, Grieve DJ, Wang M, *et al*. NADPH oxidase-4 mediates protection against chronic load-induced stress in mouse hearts by enhancing angiogenesis. *Proc Natl Acad Sci U S A* 2010; 107:18121–18126.
24. Touyz RM, Mercure C, He Y, Javeshghani D, Yao G, Callera GE, *et al*. Angiotensin II-dependent chronic hypertension and cardiac hypertrophy are unaffected by gp91phox-containing NADPH oxidase. *Hypertension* 2005; 45:530–537.
25. Burger D, Reudelhuber TL, Mahajan A, Chibale K, Sturrock ED, Touyz RM. Effects of a domain-selective ACE inhibitor in a mouse model of chronic angiotensin II-dependent hypertension. *Clin Sci (Lond)* 2014; 127:57–63.
26. Burger D, Montezano AC, Nishigaki N, He Y, Carter A, Touyz RM. Endothelial microparticle formation by angiotensin II is mediated via Ang II receptor type I/NADPH oxidase/Rho kinase pathways targeted to lipid rafts. *Arterioscler Thromb Vasc Biol* 2011; 31:1898–1907.
27. Halpern W, Mulvany MJ, Warshaw DM. Mechanical properties of smooth muscle cells in the walls of arterial resistance vessels. *J Physiol* 1978; 275:85–101.
28. Guzik TJ, Channon KM. Measurement of vascular reactive oxygen species production by chemiluminescence. *Methods Mol Med* 2005; 108:73–89.

29. Neves KB, Rios FJ, Jones R, Jeffry Evans TR, Montezano AC, Touyz RM. Microparticles from VEGF inhibitor-treated cancer patients mediate endothelial cell injury. *Cardiovasc Res* 2019; 115:978–988.
30. Valavanidis A, Vlachogianni T, Fiotakis C. 8-hydroxy-2' -deoxyguanosine (8-OHdG): a critical biomarker of oxidative stress and carcinogenesis. *J Environ Sci Health C Environ Carcinog Ecotoxicol Rev* 2009; 27:120–139.
31. Motley ED, Eguchi K, Patterson MM, Palmer PD, Suzuki H, Eguchi S. Mechanism of endothelial nitric oxide synthase phosphorylation and activation by thrombin. *Hypertension* 2007; 49:577–583.
32. Sturrock A, Cahill B, Norman K, Huecksteadt TP, Hill K, Sanders K, *et al*. Transforming growth factor-beta1 induces Nox4 NAD(P)H oxidase and reactive oxygen species-dependent proliferation in human pulmonary artery smooth muscle cells. *Am J Physiol Lung Cell Mol Physiol* 2006; 290:L661–L673.
33. Chen F, Haigh S, Barman S, Fulton DJ. From form to function: the role of Nox4 in the cardiovascular system. *Front Physiol* 2012; 3:412.
34. Nisimoto Y, Diebold BA, Cosentino-Gomes D, Lambeth JD. Nox4: a hydrogen peroxide-generating oxygen sensor. *Biochemistry* 2014; 53:5111–5120.
35. Munoz M, Martinez MP, Lopez-Oliva ME, Rodriguez C, Corbacho C, Carballido J, *et al*. Hydrogen peroxide derived from NADPH oxidase 4- and 2 contributes to the endothelium-dependent vasodilatation of intrarenal arteries. *Redox Biol* 2018; 19:92–104.
36. Zhang M, Mongue-Din H, Martin D, Catibog N, Smyrnias I, Zhang X, *et al*. Both cardiomyocyte and endothelial cell Nox4 mediate protection against hemodynamic overload-induced remodelling. *Cardiovasc Res* 2018; 114:401–408.
37. Chen K, Kirber MT, Xiao H, Yang Y, Keaney JF Jr. Regulation of ROS signal transduction by NADPH oxidase 4 localization. *J Cell Biol* 2008; 181:1129–1139.
38. Craige SM, Chen K, Pei Y, Li C, Huang X, Chen C, *et al*. NADPH oxidase 4 promotes endothelial angiogenesis through endothelial nitric oxide synthase activation. *Circulation* 2011; 124:731–740.
39. Rey FE, Cifuentes ME, Kiarash A, Quinn MT, Pagano PJ. Novel competitive inhibitor of NAD(P)H oxidase assembly attenuates vascular O (2)(-) and systolic blood pressure in mice. *Circ Res* 2001; 89:408–414.
40. Abdallah Y, Gligorievski D, Kasseckert SA, Dieterich L, Schafer M, Kuhlmann CR, *et al*. The role of poly(ADP-ribose) polymerase (PARP) in the autonomous proliferative response of endothelial cells to hypoxia. *Cardiovasc Res* 2007; 73:568–574.
41. Fonfria E, Marshall IC, Benham CD, Boyfield I, Brown JD, Hill K, *et al*. TRPM2 channel opening in response to oxidative stress is dependent on activation of poly(ADP-ribose) polymerase. *Br J Pharmacol* 2004; 143:186–192.
42. Sriram K, Laughlin JG, Rangamani P, Tartakovsky DM. Shear-induced nitric oxide production by endothelial cells. *Biophys J* 2016; 111:208–221.
43. Yada T, Shimokawa H, Hiramatsu O, Haruna Y, Morita Y, Kashihara N, *et al*. Cardioprotective role of endogenous hydrogen peroxide during ischemia-reperfusion injury in canine coronary microcirculation in vivo. *Am J Physiol Heart Circ Physiol* 2006; 291:H1138–1146.
44. Thomas SR, Chen K, Keaney JF Jr. Hydrogen peroxide activates endothelial nitric-oxide synthase through coordinated phosphorylation and dephosphorylation via a phosphoinositide 3-kinase-dependent signaling pathway. *J Biol Chem* 2002; 277:6017–6024.
45. Alves-Lopes R, Montezano AC, Neves KB, Harvey A, Rios FJ, Skiba DS, *et al*. Selective inhibition of the C-domain of ACE (angiotensin-converting enzyme) combined with inhibition of NEP (Neprilysin): a potential new therapy for hypertension. *Hypertension* 2021; 78:604–616.
46. Weil BR, Stauffer BL, Greiner JJ, DeSouza CA. Prehypertension is associated with impaired nitric oxide-mediated endothelium-dependent vasodilation in sedentary adults. *Am J Hypertens* 2011; 24:976–981.
47. Giles TD, Sander GE, Nossaman BD, Kadowitz PJ. Impaired vasodilation in the pathogenesis of hypertension: focus on nitric oxide, endothelial-derived hyperpolarizing factors, and prostaglandins. *J Clin Hypertens (Greenwich)* 2012; 14:198–205.
48. Silva GC, Silva JF, Diniz TF, Lemos VS, Cortes SF. Endothelial dysfunction in DOCA-salt-hypertensive mice: role of neuronal nitric oxide synthase-derived hydrogen peroxide. *Clin Sci (Lond)* 2016; 130:895–906.
49. Touyz RM, Alves-Lopes R, Rios FJ, Camargo LL, Anagnostopoulou A, Arner A, *et al*. Vascular smooth muscle contraction in hypertension. *Cardiovasc Res* 2018; 114:529–539.